Post-print of: Bekasiewicz A.: Model Correction and Optimization Framework for Expedited EM-Driven Surrogate-Assisted Design of Compact Antennas. IEEE ANTENNAS AND WIRELESS PROPAGATION LETTERS. Vol. 17, iss. 3 (2018), pp. 468-471. DOI: 10.1109/LAWP.2018.2795532

Model Correction and Optimization Framework for Expedited EM-Driven Surrogate-Assisted Design of Compact Antennas

Adrian Bekasiewicz, *Member, IEEE*

***Abstract*—Design of compact antennas is a numerically challenging process that heavily relies on electromagnetic (EM) simulations and numerical optimization algorithms. For reliability of simulation results, EM models of small radiators often include connectors which—despite being components with fixed dimensions—significantly contribute to evaluation cost. In this letter, a response correction method for antenna models without connector, based on a so-called network unterminating concept, has been proposed. Unterminating allows for obtaining electrical parameters of the connector embedded in the EM antenna model. They can be then utilized to refine the reflection characteristics of the EM antenna model without connector. The refined model has been optimized using a novel trust-region-based method. It exploits information gained from unsuccessful iterations to improve accuracy of the model and prevent premature convergence of the algorithm. The proposed design approach has been demonstrated using two antenna structures and compared to benchmark algorithms.**

***Index Terms*—Antenna design, connector unterminating, simulation-driven design, trust-region methods, variable-fidelity simulations.**

I. Introduction

Antennas for space-limited applications such as wearable electronics, implantable devices, or internet of things structures, have to fulfill specific performance requirements while featuring small dimensions [1]. This is normally achieved using complex geometries that can be accurately evaluated only by means of numerically expensive high-fidelity EM simulations. Also, for reliable evaluation, EM models of compact radiators often include connectors which further increase their numerical cost [2], [3].

The high cost of model evaluation makes direct EM-driven optimization of small antennas numerically impractical as conventional algorithms require hundreds of simulations to obtain the final design [3], [4]. The problem can be mitigated to some extent using a gradient-based search with cheap adjoint sensitivities [5]. However, adjoints technology is currently available in only a handful of commercial EM solvers. Surrogate-based optimization (SBO) is another group of methods that can be used to expedite the antenna design process [3], [6]. SBO shifts the optimization burden to the low-fidelity EM model that is iteratively corrected using occasionally acquired high-fidelity model data [6]-[8]. So far SBO methods such as space mapping [7], or techniques based on the concept of response features have been successfully utilized for design of small radiators [3], [8].

One of potential problems in using SBO for low-cost design of compact antennas is that their models are often equipped with connectors [2], [3], [8]. The latter, although important from the point of view of response accuracy, are static components of antenna models. In other words, connector dimensions remain unchanged in the course of antenna optimization. At the same time, it significantly contributes to model evaluation cost [3]. An attempt to mitigate this problem by conducting two stage optimization was proposed in [3]. In the first step, the antenna model without connector was optimized. The obtained design was then used as a starting point for optimization of the model with connector. However, due to inaccuracy of the first model, a large number of EM simulations was required to complete the second stage of the design process.

In this letter, a response correction method for antenna EM models without connectors based on a so-called network unterminating concept has been proposed. Unterminating allows for determining properties of the connector (in the form of $\boldsymbol{S}$-parameter matrix) embedded into the high-fidelity model of the structure. The obtained matrix data is utilized for correcting the electrical responses of the low-fidelity (connector-less) model [9]. Here, the refined coarse model is optimized within a novel, two-mode trust-region (TMTR) framework. The TMTR algorithm exploits high-fidelity data gained at unsuccessful designs to refine the surrogate and prevent premature convergence of the optimization process. The proposed algorithm has been demonstrated using two antennas and favorably compared with the benchmark algorithms.

II. Methodology

In this section, a surrogate-assisted optimization method for compact antennas design has been described, which includes the proposed response correction technique and a novel trust-region-based optimization algorithm. Numerical validation of the method is performed in Section III.

A. Problem Formulation

Let $\boldsymbol{R}_f(\boldsymbol{x})$ be the response of the high-fidelity antenna model with the connector. Also, let $A(\boldsymbol{x})$ and $E(\boldsymbol{x})$ be the antenna size and the value of its maximum in-band reflection. Here, $\boldsymbol{x}$ is the vector of structure parameters. The design problem is as follows:

$$\boldsymbol{x}^* = \arg\min_{\boldsymbol{x}} U\left(\boldsymbol{R}_f(\boldsymbol{x})\right) = \arg\min_{\boldsymbol{x}} U\left(A(\boldsymbol{x}), E(\mathrm{x})\right) \quad (1)$$

where $\boldsymbol{x}^*$ is the optimal design. The objective function is

$$U\left(A(\boldsymbol{x}), E(\boldsymbol{x})\right) = A(\boldsymbol{x}) + \beta \cdot \left(\max\{(E(\boldsymbol{x}) - E_{\max})/|E_{\max}|, 0\}\right)^2 \quad (2)$$

Manuscript submitted on October 5, 2017, revised on December 21, 2017. This work was supported by the National Science Centre of Poland Grants: 2014/15/B/ST7/04683 and 2015/17/B/ST6/01857, as well as Gdansk University of Technology Grant MNiD/2017/2018/2.

A. Bekasiewicz is with the Faculty of Electronics, Telecommunications and Informatics, Gdansk University of Technology, Poland (e-mail: bekasiewicz@ru.is).

The second term in (2) is a penalty function activated for $E(\boldsymbol{x})$ greater than $E_{\max} = -10$ dB, whereas β is the penalty factor [3].

Due to high evaluation cost of $\boldsymbol{R}_f$ model, direct solving of (1) is numerically inefficient. The problem can be mitigated using surrogate-based optimization which generates a series of approximations $\boldsymbol{x}^{(i)}$, $i = 0, 1, 2, \ldots$, to (1) by solving [6]

$$\boldsymbol{x}^{(i+1)} = \arg\min_{\boldsymbol{x}} U\left(\boldsymbol{R}_s^{(i)}(\boldsymbol{x})\right) \tag{3}$$

where $\boldsymbol{R}_s = \boldsymbol{R}_s^{(i)}$ is a low-fidelity model $\boldsymbol{R}_c$ (here, an antenna EM model without the connector) corrected by means of the $\boldsymbol{S}$-parameter matrix determined through unterminating method.

B. Response Correction Using Connector Unterminating

Connectors greatly affect operation of small radiators and thus, for the reliability of the simulation results, they have to be included in antenna EM models [3], [8]. However, including connector to the model significantly increases its evaluation cost. To address this problem, $\boldsymbol{R}_c$ can be corrected as follows [9]

$$\boldsymbol{R}_s(\boldsymbol{x}) = \frac{\boldsymbol{S}_{11} + \Delta\boldsymbol{S} \circ \boldsymbol{R}_c(\boldsymbol{x}, \boldsymbol{f})}{1 - \boldsymbol{S}_{22} \circ \boldsymbol{R}_c(\boldsymbol{x}, \boldsymbol{f})} \tag{4}$$

where $\circ$ stands for component-wise multiplication, $\boldsymbol{f}$ represents the frequency sweep for the $\boldsymbol{R}_c$ model, whereas $\boldsymbol{S}_{11}$, $\boldsymbol{S}_{22}$, and $\Delta\boldsymbol{S} = \boldsymbol{S}_{11} \circ \boldsymbol{S}_{22} - \boldsymbol{S}_{12} \circ \boldsymbol{S}_{21}$ are parameter vectors (complex-valued) of the connector embedding network. Due to the discontinuity on a connector-antenna transition, accurate values of network parameters cannot be obtained from simulations of a standalone connector EM model. Instead, they can be determined using a so-called unterminating technique, which allows for extracting parameters of the embedded two-port network from responses of a single-port device [9]. Normally, unterminating is used to improve measurement accuracy of devices connected to a network analyzer through test fixtures [9], [10]. Here, it is applied for determining the embedding network of the connector and connector-antenna transition (see Fig. 1). The network parameters are obtained from the $\boldsymbol{R}_c$ and $\boldsymbol{R}_f$ responses using the following formulas

$$\begin{aligned}
\boldsymbol{S}_{11} &= \Delta\boldsymbol{S} \circ \boldsymbol{R}_c(\boldsymbol{x}^{(1)}, \boldsymbol{f}) + \boldsymbol{R}_f(\boldsymbol{x}^{(1)}, \boldsymbol{f}) \circ (1 - \boldsymbol{S}_{22} \circ \boldsymbol{R}_c(\boldsymbol{x}^{(1)}, \boldsymbol{f})) \\
\boldsymbol{S}_{22} &= \frac{\Delta\boldsymbol{S} \circ \boldsymbol{R}_c(\boldsymbol{x}^{(2)}, \boldsymbol{f}) + \boldsymbol{R}_f(\boldsymbol{x}^{(2)}, \boldsymbol{f}) - \boldsymbol{S}_{11}}{\boldsymbol{R}_c(\boldsymbol{x}^{(2)}, \boldsymbol{f}) \circ \boldsymbol{R}_f(\boldsymbol{x}^{(2)}, \boldsymbol{f})} \\
\Delta\boldsymbol{S} &= \frac{\boldsymbol{S}_{11} - \boldsymbol{R}_f(\boldsymbol{x}^{(3)}, \boldsymbol{f}) \circ (1 - \boldsymbol{S}_{22} \circ \boldsymbol{R}_c(\boldsymbol{x}^{(3)}, \boldsymbol{f}))}{\boldsymbol{R}_c(\boldsymbol{x}^{(3)}, \boldsymbol{f})}
\end{aligned} \tag{5}$$

where $\boldsymbol{x}^{(p)}$, $p = 1, 2, 3$, ($\boldsymbol{x}^{(p)} \in \boldsymbol{X}_r$) are the reference designs (cf. Section II.*E*). Correction (4) ensures zero-order consistency between the $\boldsymbol{R}_f$ and $\boldsymbol{R}_s$ (i.e., $\boldsymbol{R}_f = \boldsymbol{R}_s^{(i)}$ for designs from $\boldsymbol{X}_r$) [6]. Comparison of the $\boldsymbol{R}_f$, $\boldsymbol{R}_c$, and $\boldsymbol{R}_s$ responses at one of the reference designs is shown in Fig. 2(a). Note that unterminating-based method is suitable only for correcting antenna reflection. Field-related figures have to be refined using other methods.

C. Two-Mode Trust-Region-Based Algorithm Framework

The surrogate model (4) is embedded in a two-mode trust-region framework, which generates a series of approximations $\boldsymbol{x}^{(i)}$, $i = 0, 1, 2, \ldots$, (here, $\boldsymbol{x}^{(0)}$ is the initial design) to the original problem (1) by solving

$$\boldsymbol{x}_t = \arg\min_{\boldsymbol{x}: \|\boldsymbol{x} - \boldsymbol{x}^{(i)}\| \le \delta^{(i)}} U\left(\boldsymbol{G}_s^{(i)}(\boldsymbol{x})\right) \tag{6}$$

The trust-region radius $\delta^{(i)}$ ($\delta^{(0)} = 1$) is updated as follows. A new design $\boldsymbol{x}^{(i+1)} = \boldsymbol{x}_t$ is accepted only for gain ratio $\rho^{(i)} > 0$ [11]. The radius is either increased for $\rho^{(i)} > 0.9$ as $\delta^{(i+1)} = \max(2.5\|\boldsymbol{x}^{(i+1)} - \boldsymbol{x}^{(i)}\|, \delta^{(i)})$ or reduced as $\delta^{(i+1)} = 0.25\|\boldsymbol{x}^{(i+1)} - \boldsymbol{x}^{(i)}\|$ when $\rho^{(i)} < 0.05$. The low cost of TMTR is ensured by replacing the surrogate $\boldsymbol{R}_s^{(i)}$ with its linear expansion model [8]

$$\boldsymbol{G}_s^{(i)}(\boldsymbol{x}) = \boldsymbol{R}_s(\boldsymbol{x}^{(i)}) + \boldsymbol{J}_s(\boldsymbol{x}^{(i)}) \cdot (\boldsymbol{x} - \boldsymbol{x}^{(i)}) \tag{7}$$

where $\boldsymbol{J}_s$ is a Jacobian of $\boldsymbol{R}_s^{(i)}$ obtained w.r.t. $\boldsymbol{x}^{(i)}$ through the finite differentiation (FD) [11]. The algorithm flow is as follows:

1. Set $i = 0$, $\delta^{(0)} = 1$, $M = 0$, add $\boldsymbol{x}^{(0)}$ to $\boldsymbol{X}$ and initialize $\boldsymbol{R}_s^{(i)}$;
2. Perform FD around $\boldsymbol{x}^{(i)}$, evaluate $\boldsymbol{R}_s^{(i)}$ to obtain $\boldsymbol{J}_s$, and construct the linear model $\boldsymbol{G}_s^{(i)}$;
3. Find $\boldsymbol{x}_t$ by solving (6) and add $\boldsymbol{x}_t$ to $\boldsymbol{X}$;
4. Compute $\rho^{(i+1)} = (\boldsymbol{R}_f(\boldsymbol{x}_t) - \boldsymbol{R}_f(\boldsymbol{x}^{(i)}))/(\boldsymbol{G}_s^{(i)}(\boldsymbol{x}_t) - \boldsymbol{G}_s^{(i)}(\boldsymbol{x}^{(i)}))$;
5. If $\rho^{(i+1)} > 0$, set $\boldsymbol{x}^{(i+1)} = \boldsymbol{x}_t$ and update the radius; else if $\rho^{(i+1)} < 0$ then (if $M = 1$, reduce radius (if $\rho^{(i)} > \rho^{(i+1)}$ set $\boldsymbol{R}_s^{(i)} = \boldsymbol{R}_s^{(i-1)}$ and $M = 0$); else set $M = 2$);
6. If $\rho^{(i+1)} \le 10^{-3} \vee \|\boldsymbol{x}^{(i+1)} - \boldsymbol{x}^{(i)}\| \le 10^{-3}$, set $\boldsymbol{x}^* = \boldsymbol{x}^{(i+1)}$ and END; otherwise set $i = i + 1$ and go to 7.
7. If $\rho^{(i)} > 0 \wedge M = 0$, update surrogate and set $M = 0$; else if $\rho^{(i)} < 0 \wedge M = 2$, reset surrogate and set $M = 1$; go to 2.

For successful iterations, TMTR works similarly to the conventional trust-region (CTR) framework [11], except that it exploits the $\boldsymbol{R}_s^{(i)}$ responses to construct the linear model [8]. When $\rho^{(i+1)} < 0$ and $M = 0$, $\boldsymbol{x}_t$ is used to reset the $\boldsymbol{R}_s^{(i)}$. This step prevents premature algorithm convergence in case of surrogate inaccuracy in the search direction. If $\rho^{(i+1)} < 0$ and $M = 1$, gain ratios obtained from $\boldsymbol{R}_s^{(i-1)}$ and $\boldsymbol{R}_s^{(i)}$ are compared. The model which provides higher ρ is then re-optimized with reduced radius. Note that all designs obtained along TMTR operation are stored in $\boldsymbol{X}$.

Numerical cost of TMTR for $\rho > 0$ is only $N + 1$ evaluations of the $\boldsymbol{R}_s$ model (here, N is the problem dimensionality). Each iteration involves one $\boldsymbol{R}_f$ simulation for verification of the design from (6). Reset of the $\boldsymbol{G}_s$ model requires only one $\boldsymbol{R}_c$ simulation at $\boldsymbol{x}_t$. Initialization of the $\boldsymbol{R}_s$ model ($i = 0$) involves two extra simulations of the $\boldsymbol{R}_c$ and $\boldsymbol{R}_f$ models.

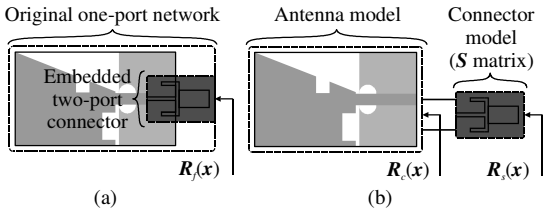

Fig. 1. The concept of connector unterminating [9]: (a) high-fidelity model of the antenna with embedded connector and (b) surrogate model obtained through correction of the connector-less low-fidelity model using $\boldsymbol{S}$-parameter matrix obtained by unterminatting procedure.

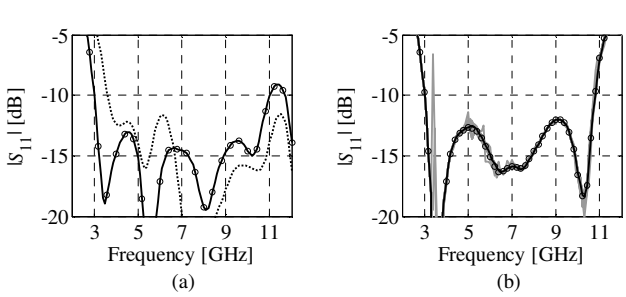

Fig. 2. Frequency responses of an exemplary antenna structure: (a) obtained for $\boldsymbol{R}_c$ (···), $\boldsymbol{R}_f$ (—), and $\boldsymbol{R}_s$ (○) models at the reference design; (b) selection of the surrogate with the lowest $E_{k.n}$ (○) among all $\boldsymbol{R}_{s.k}$ surrogates (gray lines) evaluated at perturbation $\boldsymbol{x}_n^{(i)}$. Note that responses of the selected $\boldsymbol{R}_s(\boldsymbol{x}_n^{(i)})$ surrogate (○) and the $\boldsymbol{R}_f(\boldsymbol{x}^{(i)})$ model (black line) are very similar.

D. Selecting Surrogates for TMTR optimization

Although the $\boldsymbol{R}_s$ model is locally accurate, the matrix obtained from (5) may contain non-physical values (i.e., greater than one) resulting from differences between the designs in the reference set $\boldsymbol{X}_r$. These local errors may result in fluctuations of model responses (see Fig. 2(b)) and, consequently, worsen the TMTR performance. To mitigate this problem, the algorithm evaluates a series of $\boldsymbol{R}_{s.k}$ surrogates (k = 1, …, K), constructed using different reference sets $\boldsymbol{X}_r = \boldsymbol{X}_{r.k}$ ($\boldsymbol{X}_{r.k} \subset \boldsymbol{X}$). These sets consist of designs obtained in previous algorithm iterations (cf. Section II.*E*), thus the construction of $\boldsymbol{R}_{s.k}$ models does not increase the optimization cost. Because TMTR exploits $\boldsymbol{R}_{s.k}$ surrogates only for FD, it is expected that $E_{k.n} = \|\boldsymbol{R}_f(\boldsymbol{x}^{(i)}) - \boldsymbol{R}_{s.k}(\boldsymbol{x}_n^{(i)})\|_2$, where $\boldsymbol{x}_n^{(i)}$ is the perturbation of $\boldsymbol{x}^{(i)}$ along the dimension n (n = 1, …, N), is small. Therefore, for each $\boldsymbol{x}_n^{(i)}$, the $\boldsymbol{R}_{s.k}$ surrogate for which $E_k = \min(E_{1.n}, \ldots E_{K.n})$ is selected as $\boldsymbol{R}_s(\boldsymbol{x}_n^{(i)})$. Note that the risk of using distorted responses for the $\boldsymbol{G}_s^{(i)}$ construction gradually decreases, because the number of $\boldsymbol{R}_{s.k}$ models grows with TMTR iterations. Exemplary responses of all $\boldsymbol{R}_{s.k}$ surrogates, as well as reflection characteristics of the $\boldsymbol{R}_f$ model and the selected $\boldsymbol{R}_s(\boldsymbol{x}_n^{(i)})$ models at certain design $\boldsymbol{x}^{(i)}$ are shown in Fig. 2(b).

E. Reference Designs for Connector Unterminating

The way of selecting reference designs $\boldsymbol{x}^{(j)}$, j = 1, …, J, ($\boldsymbol{x}^{(j)} \in \boldsymbol{X}$) to 3-element sets depends on the TMTR algorithm step. In the first iteration, a set containing the initial design and two points located around it, is used. If $\rho^{(i)} > 0$, $\boldsymbol{X}_{r.1} = \{\boldsymbol{x}^{(1)}, \boldsymbol{x}^{(2)}, \boldsymbol{x}^{(J)}\}$, $\boldsymbol{X}_{r.2} = \{\boldsymbol{x}^{(1)}, \boldsymbol{x}^{(3)}, \boldsymbol{x}^{(J)}\}$, …, $\boldsymbol{X}_{r.K} = \{\boldsymbol{x}^{(J-2)}, \boldsymbol{x}^{(J-1)}, \boldsymbol{x}^{(J)}\}$, $K = C(J - 1, 2)$, sets are constructed. If $\rho^{(i)} < 0$ and $M = 2$, $\boldsymbol{X}_{r.k} = \{\boldsymbol{x}^{(k)}, \boldsymbol{x}^{(J-1)}$, and $\boldsymbol{x}^{(J)}\}$, k = 1, …, $J - 2$, sets are generated.

III. Case Studies

In this section, the surrogate model and the optimization framework introduced in Section II are demonstrated using two test antennas. Both structures are implemented on a Taconic RF-35 substrate (ε_r = 3.5, tanδ = 0.0018, h = 0.762 mm). The antennas are optimized using (2), i.e., for size reduction while maintaining in-band reflection level below –10 dB.

A. Bandwidth-Enhanced Patch

The first example is the antenna shown in Fig. 3. It consists of a monopole connected to a patch radiator with inset feed and trimmed ground plane. The input impedance is 50 Ω. The design variables are $\boldsymbol{x} = [L\ l_2\ W\ w_2\ l_0\ o_0]^T$, whereas $o = L/4.5$, $l_s = 0.1L$ are relative and l_1 = 1.5, w_1 = 2.5, w_s = 0.5, w_0 = 1.7 are fixed (all in mm). The vector of adjustable parameters has been selected based on sensitivity analysis of antenna responses [6]. The connector-equipped model $\boldsymbol{R}_f$ (~400,000 cells, average simulation time on a dual Intel Xeon E5540: 110 s) and connector-less model $\boldsymbol{R}_s$ (~100,000 cells, simulation time: 35 s) are both implemented in CST Studio and evaluated using its time domain (TD) solver [12]. The antenna footprint is $A(\boldsymbol{x}) = (l_2 + 2o_0)\cdot(l_0 + L + w_2 + o_0 + l_1)$, whereas $E(\boldsymbol{x}) = \max\{|S_{11}|_{5\ \text{GHz to}\ 6\ \text{GHz}}\}$. The lower and upper bounds are: $\boldsymbol{l} = [10\ 5\ 3.5\ 0.2\ 3\ 2]^T$ and $\boldsymbol{u} = [25\ 25\ 10\ 3.2\ 15\ 10]^T$.

The size of the antenna at the initial design $\boldsymbol{x}^{(0)} = [19.92\ 11.82\ 4.12\ 0.4\ 9.89\ 10]^T$ is 1327 mm^2. The design has been obtained through optimization of the antenna for the best in-band matching. The final design $\boldsymbol{x}^* = [19.06\ 13.38\ 3.5\ 1.46\ 4.86\ 2]^T$ has been found in 15 iterations of the algorithm of Section II. The resulting antenna size is only 507 mm^2 (62% miniaturization w.r.t. $\boldsymbol{x}^{(0)}$). A comparison of the $\boldsymbol{R}_c$ and $\boldsymbol{R}_f$ model performance characteristics at both designs and responses of the $\boldsymbol{R}_f$ model evaluated—for the sake of validation—using finite elements method (FEM) is shown in Fig. 4. The vertical misalignment between the responses obtained using both solvers is acceptable.

The TMTR algorithm has been compared to conventional trust-region approach [11] and a pattern search [13], both exploiting only $\boldsymbol{R}_f$ model simulations. To justify the usefulness of the TMTR reset mechanism, the surrogate has also been optimized using CTR with $\boldsymbol{R}_s$. The starting point for all algorithms was $\boldsymbol{x}^{(0)}$. Table I compares algorithms in terms of number of simulations, cost (w.r.t. number of $\boldsymbol{R}_f$ evaluations and absolute time), and performance. The results indicate that the cost of TMTR is over two fold lower compared to CTR. Owing to exploitation of unsuccessful designs for refinement, final design obtained using TMTR is significantly smaller than the one obtained by CTR with $\boldsymbol{R}_s$. Also, the cost TR-based methods is an order of magnitude lower compared to pattern search.

B. Antenna II

Consider a ultra-wideband (UWB) monopole shown in Fig. 5 [14]. It consists of a trapezoid radiator with two rectangular slits fed through a microstrip line and a modified ground plane with an elliptical slot. The design parameters are: $\boldsymbol{x} = [l_0\ l_1\ w_{1r}\ w_2\ o_{1r}\ o_{2r}\ o_{3r}\ s_{1r}\ s_{2r}\ s_{4r}\ s_{5r}\ g]^T$. Dimension w_0 = 1.7 is fixed to ensure 50 Ohm input impedance, whereas $w_1 = (0.5w_2 - 0.5w_0)w_{1r}$, $o_2 = 0.5w_2o_{2r}$, $o_3 = (l_1 - s_3)o_{3r}$, $s_1 = (0.5w_2 - 0.5w_0)s_{1r}$, $s_2 = l_1s_{2r}$, $s_4 = (w_2 - 2s_5)s_{4r}$, and $s_5 = 0.5(l_0 - g)s_{5r}$ are relative. The parameters without r in subscript are in mm. The structure models $\boldsymbol{R}_f$ (with connector, 6,000,000 cells, simulation time: 30 min) and $\boldsymbol{R}_c$ (without connector, 1,500,000 cells, simulation time: 5 min) are implemented in CST Microwave Studio. The antenna size and in-band reflection are $A(\boldsymbol{x}) = w_2\cdot(l_1 + l_0)$ and $E(\boldsymbol{x}) = \max\{|S_{11}|_{3.1\ \text{GHz to}\ 10.6\ \text{GHz}}\}$. The search space bounds are: $\boldsymbol{l} = [4\ 3\ 0\ 4\ 0\ 0\ 0\ 0\ 0.1\ 0\ 0.01\ 0.01\ 0]^T$ and $\boldsymbol{u} = [24\ 24\ 1\ 24\ 1\ 0.5\ 1\ 0.9\ 0.3\ 0.5\ 0.5\ 2]^T$.

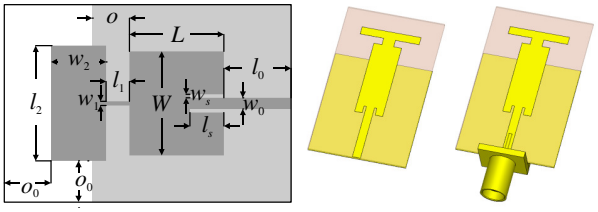

(a) (b) (c)

Fig. 3. A bandwidth-enhanced patch: (a) antenna parameterization, as well as visualizations of (b) connector-less, and (c) connector-equipped EM models.

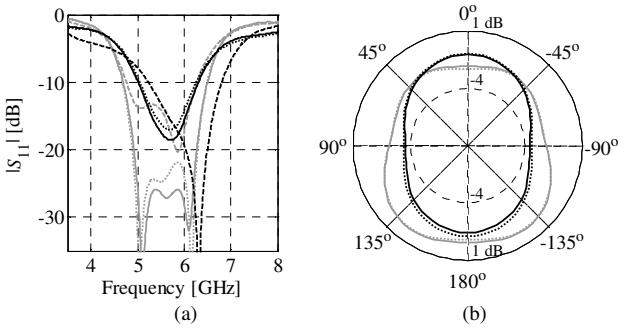

(a) (b)

Fig. 4. The patch antenna: (a) reflection responses of the $\boldsymbol{R}_f$ (—) and $\boldsymbol{R}_c$ (– –) models at the $\boldsymbol{x}^{(0)}$ (gray) and $\boldsymbol{x}^*$ (black) designs, and (b) E-plane gain patterns obtained for the 5.5 GHz frequency at $\boldsymbol{x}^{(0)}$ (gray) and $\boldsymbol{x}^*$ (black) designs. Dotted lines denote responses obtained from $\boldsymbol{R}_f$ model evaluations using FEM solver.

The initial design $\boldsymbol{x}^{(0)}$ = [8.66 17.23 0.23 16.8 0.23 0 0.18 0.88 0.04 0.08 0.32 0.5]^T has been obtained through minimization of the antenna reflection. The antenna size at $\boldsymbol{x}^{(0)}$ is 434 mm^2. The final design $\boldsymbol{x}^*$ = [9.32 14.77 0.23 13.11 0.22 0 0.18 0.88 0.06 0.08 0.33 0.48]^T has been found after 10 iterations of TMTR algorithm. The antenna dimensions at $\boldsymbol{x}^*$ are 13.1 mm × 24.1 mm (footprint: 316 mm^2) and the obtained miniaturization rate is 27%. Frequency characteristics from $\boldsymbol{R}_c$ and $\boldsymbol{R}_f$ models simulations, as well as from evaluation of $\boldsymbol{R}_f$ model using FEM solver obtained for $\boldsymbol{x}^{(0)}$ and $\boldsymbol{x}^*$ designs are compared in Fig. 6(a). Misalignment between TD- and FEM-based responses is acceptable. Table II compares the TMTR with benchmark algorithms. For the considered antenna, the optimization cost of TMTR is 72% and 10% lower than for CTR and CTR with $\boldsymbol{R}_s$ surrogate, respectively. At the same time, the final design found by TMTR is almost 10% smaller compared to the one found by CTR with $\boldsymbol{R}_s$. The in-band reflection at $\boldsymbol{x}^*$ is similar for all considered algorithms. Numerical cost of pattern search is from 5.8 to 21 times higher compared to gradient-based methods considered here.

Convergence plots obtained for gradient-based methods are shown in Fig. 6(b). Among compared algorithms, TMTR requires the smallest number of iterations to complete the optimization process. Note that the convergence plots for TMTR and CTR with $\boldsymbol{R}_s$ do not fall below 10^{-3} threshold. This is because, for both algorithms, the $\rho \le 10^{-3}$ condition has been fulfilled beforehand.

TABLE I PATCH ANTENNA OPTIMIZATION: COST BREAKDOWN

Considered algorithms	No. of model evaluations		Optimization cost		Antenna size at $\boldsymbol{x}^*$	max($\lvert S_{11}\rvert$) in-band at $\boldsymbol{x}^*$
	$\boldsymbol{R}_c$	$\boldsymbol{R}_f$	$\boldsymbol{R}_f$	hours	[mm^2]	[dB]
TMTR (this work)	67	18	39.3	1.20	507	–9.8
CTR with $\boldsymbol{R}_s$	63	19	39.0	1.19	686	–9.9
CTR [11]	N/A	89	89.0	2.72	470	–9.9
Pattern search [13]	N/A	583	583.0	17.8	505	–10.0

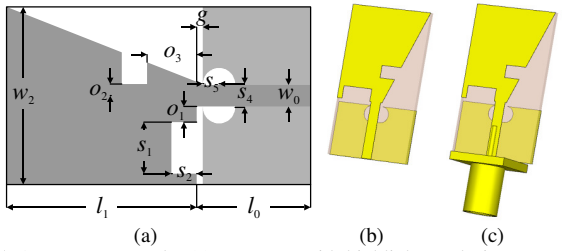

Fig. 5. A UWB monopole: (a) geometry with highlight on design parameters, as well as visualizations of models with (b), and without connector (c).

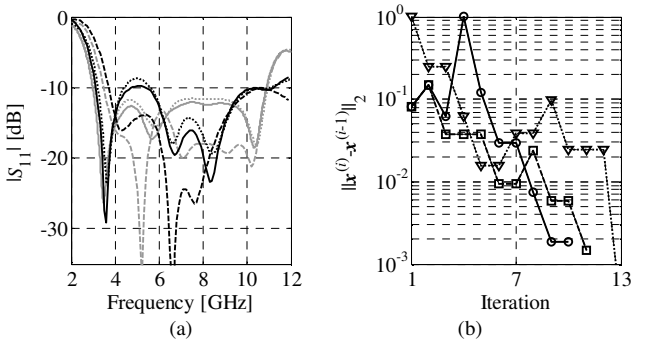

Fig. 6. The UWB monopole: (a) reflection responses of the $\boldsymbol{R}_f$ (—) and $\boldsymbol{R}_c$ (– –) models, as well as the $\boldsymbol{R}_f$ model evaluated using FEM solver (···) at the $\boldsymbol{x}^{(0)}$ (gray) and $\boldsymbol{x}^*$ (black) designs; (b) convergence plots of TMTR (○), CTR with $\boldsymbol{R}_s$ (□), and CTR (▽).

TABLE II UWB MONOPOLE OPTIMIZATION: COST BREAKDOWN

Considered algorithms	No. of model evaluations		Optimization cost		Antenna size at $\boldsymbol{x}^*$	max($\lvert S_{11}\rvert$) in-band
	$\boldsymbol{R}_c$	$\boldsymbol{R}_f$	$\boldsymbol{R}_f$	hours	[mm^2]	at $\boldsymbol{x}^*$ [dB]
TMTR (this work)	84	13	34.0	11.3	316	–9.8
CTR with $\boldsymbol{R}_s$	94	14	37.5	12.5	345	–9.9
CTR [11]	N/A	121	121.0	40.3	291	–9.9
Pattern search [13]	N/A	705	705.0	235	341	–10.0

IV. CONCLUSION

In this letter, a response correction method for fast and accurate optimization of connector-less models of compact antennas based on unterminating concept has been proposed. The corrected surrogate model has been embedded in a modified trust-region framework that exploits information gained from unsuccessful iterations to prevent premature convergence of the optimization process. The approach has been demonstrated using two test cases: a bandwidth enhanced patch and a UWB monopole. For the considered structures, the proposed model correction/design optimization approach features similar performance as conventional trust-region algorithm executed on models with connectors, yet its computational cost is up to 70 percent lower. Future work will focus on adaptation of the method for structures with the connector and housing. Development of design approaches for correcting field and electrical figures of connector-less EM models will be also considered.

ACKNOWLEDGMENT

The author would like to thank prof. Slawomir Koziel (Reykjavik University, Iceland) for making CST Studio available.

REFERENCES

[1] M. Ur-Rehman, Q.H. Abbasi, M. Akram, C. Parini, "Design of band-notched ultra wideband antenna for indoor and wearable wireless communications," *IET Microwaves, Ant. Prop.*, vol. 9, no. 3, pp. 243-251, 2015.

[2] M.S. Khan, A.-D. Capobianco, A. Iftikhar, S. Asif, and B.D. Braaten, "A compact dual polarized ultrawideband multiple-input- multiple-output antenna," *Microw. Opt. Tech. Lett.*, vol. 58, no. 1, pp. 163-166, 2016.

[3] A. Bekasiewicz and S. Koziel, "Structure and computationally-efficient simulation-driven design of compact UWB monopole antenna," *IEEE Ant. Wireless Prop. Lett.*, vol. 14, pp. 1282-1285, 2015.

[4] S. Koziel and S. Ogurtsov, "Design optimization of antennas using electromagnetic simulations and adaptive response correction technique," *IET Microwaves, Ant. Prop.*, vol. 8, no. 3, pp. 180-185, 2014.

[5] S. Koziel, F. Mosler, S. Reitzinger, and P. Thoma, "Robust microwave design optimization using adjoint sensitivity and trust regions," *Int. J. RF and Microwave CAE*, vol. 22, no. 1, pp. 10-19, 2012.

[6] S. Koziel, and S. Ogurtsov, *Antenna design by simulation-driven optimization*, Springer, 2014.

[7] S. Koziel, Q.S. Cheng, and J.W. Bandler, "Space mapping," *IEEE Microwave Mag.*, vol. 9, no. 6, pp. 105–122, 2008.

[8] S. Koziel and A. Bekasiewicz, "Expedited simulation-driven design optimization of UWB antennas by means of response features," to appear, *Int. J. RF Microwave CAE*, 2017.

[9] R.F. Bauer and P. Penfield, "De-Embedding and unterminating," *IEEE Trans. Microwave Theory Techn.*, vol. 22, no. 3, pp. 282-288, 1974.

[10] D. Williams, "De-embedding and unterminating microwave fixtures with nonlinear least squares," *IEEE Trans. Microwave Theory Techn.*, vol. 38, no. 6, pp. 787-791, 1990.

[11] A. Conn, N.I.M. Gould, P.L. Toint, *Trust-region methods*, MPS-SIAM Series on Optimization, Philadelphia, 2000.

[12] CST Microwave Studio, ver. 2013, Dassault Systems, France 2013.

[13] S. Koziel, "Computationally efficient multi-fidelity multi-grid design optimization of microwave structures," *Applied Comp. EM Soc. J.*, vol. 25, no. 7, pp. 578-586, 2010.

[14] S.K. Palaniswamy, Y. Panneer, M.G. Nabi Alsath, M. Kanagasabai, S. Kingsly, and S. Subbaraj, "3D eight-port ultra-wideband (UWB) antenna array for diversity applications," *IEEE Ant. Wireless Prop. Lett.*, vol. 16, pp. 569-572, 2017.